A Computer Modeling of Mie-Scattering by Spherical Droplets Within the Atmosphere

Mohsen Javaherian[1] · Bahram Abedi Ravan[2]

[1] Department of Physics, University of Zanjan, Zanjan, P.O. Box 45195313, Iran [2] Faculty of Basic Sciences, Shahid Sattari Aeronautical University of Science and Technology, P.O. Box 13846-63113, Tehran, Iran

Abstract. The Earth's atmosphere is an environment replete with particles of different sizes with various refractive indices which affect the light radiation traveling through it. The Mie scattering theory is one of the well-known light scattering techniques applicable to modeling of electromagnetic scattering from tiny atmospheric particles or aerosols floating in the air or within the clouds. In this study, the scattering characteristics of atmospheric particles are investigated for a wide range of particle types and particle sizes within the framework of Mie's theory. The scattering and back-scattering coefficients are calculated and it is observed that the maximum scattering occurs for particle sizes comparable to the radiation wavelength while the spherical particles with diameters much greater than the wavelength scatter the least. The calculations were carried out in the MATLAB environment and the results demonstrate that the scattering anisotropy has a direct relation with diameter of the particles.

Keywords: Light Scattering, Electromagnetic Absorption, Mie theory

1 Introduction

In the field of light scattering studies, one of the important problems that has exact solution is the theory of absorption and scattering by small spherical particles with specific radius and refractive index [1]. The basis computations for this kind of scattering was proposed by Gustav Mie (1908) when he tried to understand scattering of light by small gold particles suspended in water [2]. Concurrently, Peter Debye was working on radiation scattered by particles in the interstellar medium [3]. But, neither Mie nor Debye were able to formulate the exact mechanism of scattering by spheroids. Historical evidences reveal that it was Lorenz who later found the solution; though, nowadays, the theory is commonly known as Mie theory [4]. In Mie's scattering theory, wavelength of the incident radiation has to be slightly less than or equal to dimensions of the particle and the particle's refractive index is supposed to be greater than that of the surrounding environment.

By now, vast numbers of research papers and valuable reviews and books are published on the subject of describing or applying Mie's theory [5, 6, 7, 8, 9]. Nowadays, the theory finds broad range of applications in areas such as studying scattering caused by interstellar dust, near-field optics and pertinent engineering subjects [10]. Vast number of official and unofficial program packages can be found which are written with the intention of simulating the Mie scattering. Specifically, it is incorporated in state-of-the-art applied softwares such as MATLAB and COMSOL. For further details, the readers are referred to Mätzler (2002), Kolwas (2010), and Yushanov et al. (2013).

There are primary works which have exploited Mie's theory to investigate the light scattering and transmission by droplets. Stratton and Houghton (1931) demonstrated that the

size of droplets is a factor that controls the transmission characteristics in the fog. They presented that their theoretical transmission curves has correspondence with experimental results [14]. In other work, the scattering cross section of droplets were discussed by Houghton and Chalker (1949). They defined the parameter $\alpha = \frac{2\pi r}{\lambda}$, which is known as dimensionless size parameter [7] (see Section 3), to plot the scattering area coefficient versus this parameter [15]. In the range that they picked up for α, it was appeared some minima and maxima indicated the behavior oscillation. The amplitude of scattering area coefficient decreased with increasing α. In one of the recent works, Mie's scattering theory has been employed to calculate the maximum value of the polarized phase function for spherical particles with regard to their bimodal log-normal size distribution [16]. The maximum value of the polarized phase function for spheroids in the atmosphere with randomly oriented was calculated using polarized sun-photometer measurements. In comparison, both experimental and analytical results did not show a significant difference.

For droplets floating in atmosphere, their shape naturally requires to have the minimum amount of surface tension in specific volume. So, it tends to arrive at optimum state of the surface area which leads to spherical shapes for drops within atmosphere. Thus, it seems that the use of Mie's theory for scattering made by droplets is a good approximation.

The amount of water per unit volume, which depends on various parameters, is changing in various parts of the atmosphere throughout different layers. The first thing that is influenced by density of water (humidity) is the size of droplets. Since the size of droplets affects light scattering, we decided to compute both forward and backward scattering using analytical simulation. This can present the values of scattering efficiencies wherever throughout the lower layers of the atmosphere depending on humidity. Moreover, this technique can be used for planets with atmosphere including tiny particles (vapors) such as Mars and Saturn [17, 18].

In this work, we have applied the Mie scattering techniques to scattering analysis of an incident electromagnetic wave by particles of various sizes. The analytical solutions are implemented in the MATLAB environment. The scattering coefficients and anisotropy parameters are obtained via simulation and the results are verified by comparison to the extract electromagnetic wave behavior of a target placed in different atmospheric conditions.

The paper is organized as follows: A concise description of the fundamental formulations of Mie's theory is expressed in Section 2. The investigation results are presented and discussed in Section 3. Section 4 summarizes our achievements and proposes an outlook for future studies.

2   Mie Theory of Light Scattering by a Sphere

We know that a time dependent electromagnetic field in a linear, homogeneous and isotropic medium satisfies the following wave equations

$$\nabla^2 \mathbf{E} + k^2 \mathbf{E} = 0; \qquad \nabla^2 \mathbf{H} + k^2 \mathbf{H} = 0, \tag{1}$$

with $k^2 = \omega^2 \mu \epsilon$ where ω is frequency of the incident wave, μ is the magnetic permeability and ϵ is the electric permittivity. Since the charge density is zero, we would have

$$\boldsymbol{\nabla}.\mathbf{E} = 0, \quad \boldsymbol{\nabla}.\mathbf{H} = 0. \tag{2}$$

Moreover, according to Maxwell's equations, and on the basis of Faraday's and Ampère's laws,

$$\boldsymbol{\nabla} \times \mathbf{E} = i\omega\mu\mathbf{H}, \quad \boldsymbol{\nabla} \times \mathbf{H} = -i\omega\mu\mathbf{E}. \tag{3}$$
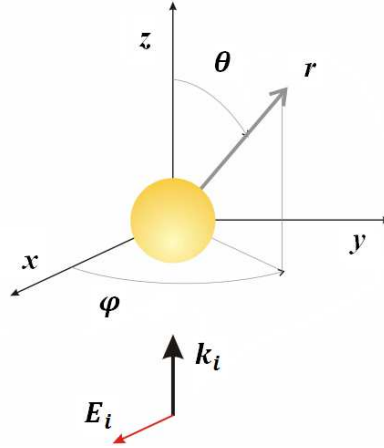
Figure 1: The geometry of the scattering problem is shown in the spherical coordinates.

To solve Eq. (1), we must find a solution for wave function expressed as follows

$$\nabla^2 \psi + k^2 \psi = 0, \tag{4}$$

where ψ is a scaler parameter called the *Generating Function* [19].

To find a convenient solution for Eq. (4), the use of spherical coordinates is needed, because the geometry of an isolated particle illustrates the spherical symmetry (See Figure 1). In this coordinates, the differential form of the scalar wave equation can be written as

$$\frac{1}{r^2}\frac{\partial}{\partial r}\left(r^2\frac{\partial\psi}{\partial r}\right) + \frac{1}{r^2\sin\theta}\frac{\partial}{\partial\theta}\left(\sin\theta\frac{\partial\psi}{\partial\theta}\right) + \frac{1}{r^2\sin\theta}\frac{\partial^2\psi}{\partial^2\varphi} + k^2\psi = 0. \tag{5}$$

By substituting the solution $\psi(r,\theta,\varphi) = R(r)\Theta(\theta)\Phi(\varphi)$, three separate equations will be yielded which are linearly independent and single-valued. Thus, the complete solution of Eq. (5) takes the following forms

$$\psi_{emn}(r,\theta,\varphi) = \cos m\varphi P_n^m(\cos\theta)z_n(kr), \tag{6}$$

$$\psi_{omn}(r,\theta,\varphi) = \sin m\varphi P_n^m(\cos\theta)z_n(kr), \tag{7}$$

where subscripts e and o are representatives of *evenness* and *oddness*, respectively. In this formula, P_n^m are the *associated Legendre functions* where the integers n and m denote the degree and the order number, respectively. Depending on the problem conditions, z_n with argument k can be any of the four spherical *Bessel* functions. The solution of Eq. (4) has a capability of being expanded as an infinite series of the functions (6) and (7) [1, 19].

In the spherical coordinates, an incident electromagnetic plane wave which is linearly polarized along the x axis and is propagating in the z direction (Figure 1) can be expressed as

$$\mathbf{E}_i = E_0 \exp(ikr\cos\theta)\mathbf{e}_x, \tag{8}$$

where E_0 and k are the amplitude of the electric field and the wavenumber, respectively. The unit vector, $\mathbf{e}_x$, lies in the polarization direction and takes the following form in the spherical coordinates

$$\mathbf{e}_x = \sin\theta\cos\varphi\mathbf{e}_r + \cos\theta\cos\varphi\mathbf{e}_\theta - \sin\theta\mathbf{e}_\varphi. \tag{9}$$

Considering the boundary conditions between the particle and its surroundings, we have

$$(\mathbf{E}_i + \mathbf{E}_s - \mathbf{E}_l) \times \mathbf{e}_r = (\mathbf{H}_i + \mathbf{H}_s - \mathbf{H}_l) \times \mathbf{e}_r$$
$$= 0. \tag{10}$$

The notations E_s and H_s are used for scattered electric and magnetic fields, respectively. On the other hand, the electric and magnetic fields inside the particle are indicated by E_l and H_l, respectively. Using some algebraic calculations, orthogonality conditions, and with the help of boundary conditions, the unknown coefficients of the spherical harmonics form of Eq. (8) are computed by using the spherical Hankel functions of the first kind, $H_n^{(1)}$.

Mie coefficients for the scattered field are introduced as the coefficients a_n and b_n. Then, using Eq. (10), at the surface of the sphere, the analytical solution for the Mie coefficients are extracted

$$a_n = \frac{\mu m^2 J_n(mx)[xJ_n(x)]' - \mu_l m^2 J_n(x)[mxJ_n(mx)]'}{\mu m^2 J_n(mx)[xH_n^{(1)}(x)]' - \mu_l H_n^{(1)}(x)[mxJ_n(mx)]'}, \tag{11}$$

$$b_n = \frac{\mu_l J_n(mx)[xJ_n(x)]' - \mu J_n(x)[mxJ_n(mx)]'}{\mu_l J_n(mx)[xH_n^{(1)}(x)]' - \mu H_n^{(1)}(x)[mxJ_n(mx)]'}. \tag{12}$$

Parameters μ and μ_l are the magnetic permeabilities of the medium and the spherical particle, respectively. Parameter x, which is defined as $x = kr = \frac{2\pi R n}{\lambda}$, is named the size parameter, wherein R and λ are the radius of the sphere and the incident wavelength, respectively. Parameter m is the proportion of the refractive index of the particle to refractive index of the surrounding medium, (*i.e.,* $m = \frac{n_l}{n}$). The superscript " $\prime$ " means derivative with respect to the mentioned argument. The index n is ranged from 1 to ∞, but the infinite series appeared in Mie relations can be truncated at a value n_{max}, which is proposed by Bohren and Huffman (1983)

$$n_{max} = x + 4x^{\frac{1}{3}} + 2. \tag{13}$$

There is another condition which states that the coefficients must vanish for all $m \neq 1$ within the particle. So, using the boundary condition expressed in Eq. (10), the coefficients c_n and d_n, and hence, the internal fields can be attainable inside the sphere in the same way as described for the external fields

$$c_n = \frac{\mu_l J_n(x)[xH_n^{(1)}(x)]' - \mu_l H_n^{(1)}(x)[xJ_n(x)]'}{\mu_l J_n(mx)[xH_n^{(1)}(x)]' - \mu H_n^{(1)}(x)[mxJ_n(mx)]'}, \tag{14}$$

$$d_n = \frac{\mu_l m J_n(x)[xH_n^{(1)}(x)]' - \mu_l m H_n^{(1)}(x)[xJ_n(x)]'}{\mu m^2 J_n(mx)[xH_n^{(1)}(x)]' - \mu_l H_n^{(1)}(x)[mxJ_n(mx)]'}. \tag{15}$$

For detailed information about the algebra and related programming, the readers are referred to Bohren and Huffman (1983), Mätzler (2002), and García-Cámara (2010). We seek both the scattering efficiency Q_{scat} (*i.e.,* the scattered light power integrated over all directions) and the extinction efficiency Q_{ext} by the *Extinction Theorem* [20] that leads to

$$Q_{scat} = \frac{2}{x^2} \sum_{n=1}^{\infty} (2n+1) \left(|a_n|^2 + |b_n|^2 \right), \tag{16}$$

$$Q_{ext} = \frac{2}{x^2} \sum_{n=1}^{\infty} (2n+1) Re\left(a_n + b_n \right). \tag{17}$$

where the index n runs up to n_{max}, the series truncation number, as given in Eq. (13).

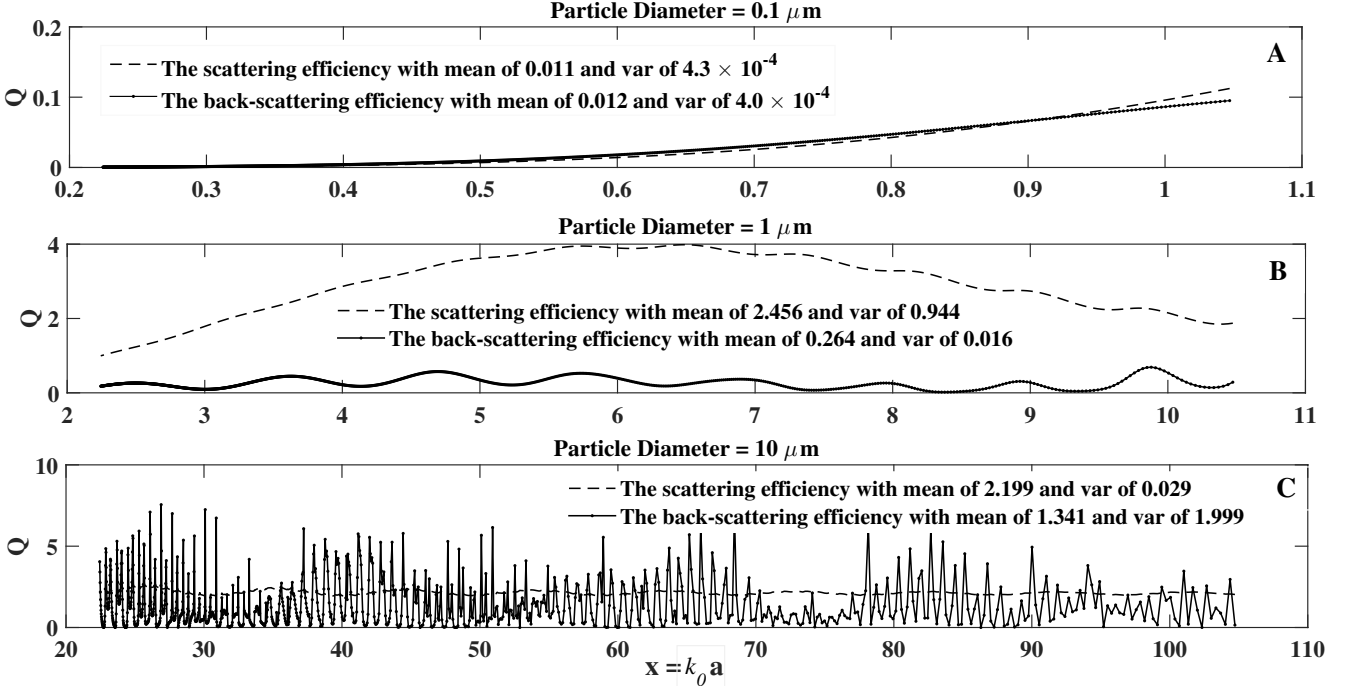Figure 2: The scattering (dashed lines) and back-scattering (solid lines) efficiencies with their mean and variance for particles with diameters 0.1 μm (A), 1 μm (B), and 10 μm (C). The incident wavelengths are ranged from 0.3 to 1.4 μm represented by dimensionless size parameter $\mathbf{x}$. The parameter a is radius of the spherical particle and the wavenumber k_0 is defined as $\frac{2\pi}{\text{wavelength}}$.

During the interaction between light and particle, the energy conservation dictates that the scattering and the absorption efficiencies add up to the extinction efficiency

$$Q_{ext} = Q_{scat} + Q_{abs}. \tag{18}$$

Another important parameter, which is applicable to monostatic radars, is the back-scattering efficiency Q_b [20] that has the following form

$$Q_b = \frac{1}{x^2} | \sum_{n=1}^{\infty} (2n+1)(-1)^n (a_n - b_n) |^2. \tag{19}$$

3   Results and Discussion

Using Eqs. (11)–(19), the programs are prepared to be performed in the MATLAB environment. To do this, the refractive index of the surrounding medium and the spherical droplet are assumed to be 1 and $\frac{4}{3}$, respectively. Both the surrounding medium and the droplet are taken to be nonmagnetic and their magnetic permeabilities are set equal to 1. First, the dimensionless size parameter is defined as $\mathbf{x} = \frac{2\pi a}{\lambda}$, where the parameters a and λ are the radius of particle and wavelength, respectively [7, 15]. Then, the scattering and
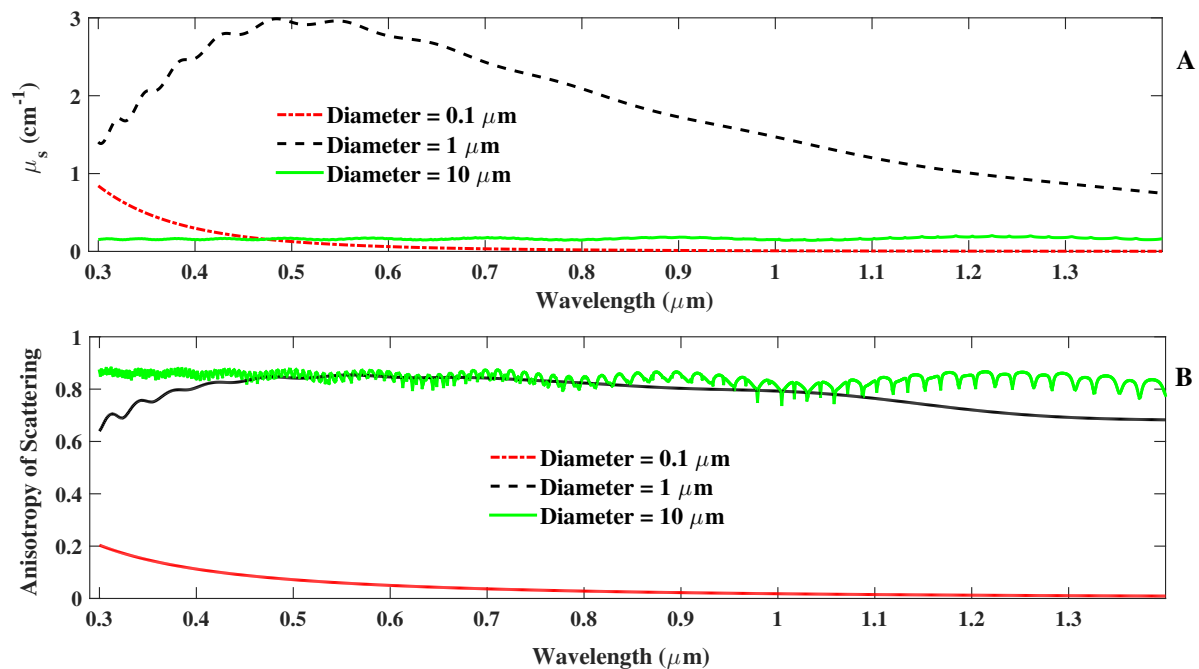
Figure 3: The scattering coefficient for particle with three different diameters (*i.e.*, 0.1, 1, and 10 μ m) for long range of wavelengths ([0.3 1.4] μm) in steps of 0.001 μm is drawn (A). As it can be seen the scattering coefficient for particles with 1 μ m (black dashed line) takes values greater than that of other size of particles. The anisotropy of scattering for particle with three different diameters for wavelengths ranged from 0.3 μm to 1.4 μm is extracted (B). This parameter shows that how the scattering made by droplets in different directions is influenced by the size of particle.

back-scattering efficiencies are computed for particles with three different diameters of 0.1, 1, and 10 μm where the incident wavelength is incremented from 0.3 to 1.4 μm (covering the whole visible spectrum) in steps of 0.001 μm (Figure 2). As it can be seen in Figure 2A, both the scattering and back-scattering efficiencies follow the same ascending behavior when the particle size is smaller than the wavelength. The range of scattering and back-scattering efficiencies is completely separated when the particle size is comparable to the wavelength (Figure 2B). For particle size comparable with incident wavelengths, the role of spherical harmonics (as discussed in Houghton and Chalker (1949)) is better appeared as smoothed fluctuations in both efficiencies specially in the back-scattering efficiency. In the case of the droplet being larger than the wavelength, the back-scattering efficiency fluctuates considerably while the scattering follows an almost straight line for all wavelengths (Figure 2C). The variance of scattering efficiency of particles having diameters more greater than the incident wavelengths displays that it approximately follows the same trend.

For the next step, we are interested in obtaining the scattering coefficient μ_s defined as

$$\mu_s = 10000\, \rho\, Q_{scat}A, \quad \text{where} \quad \rho = \frac{F_v}{V_{sphere}}. \tag{20}$$

Here, A is the geometrical cross section of the spherical particle with a dimension of [μm^2]. The variable ρ, known as the concentration of spheres inside the given volume of the sur-

rounding, has a dimension of $[\mu m^{-3}]$. Parameter V_{sphere} is the volume of sphere, and F_v is a volume fraction of spheres in the medium (a criterion for humidity). In our example, the level of humidity in the medium is considered to be 0.05 kgm^{-3} ($F_v = 0.00005$). This value roughly imitates the highest possible humidity occurring in the atmosphere.

The scattering coefficient, as defined in Eq. 20, represents a criterion for measuring the amount of scattering per spatial unit (*e.g.*, m, cm). In Figure 3A, it can be observed that the scattering coefficient decreases for all particle sizes as the incident wavelength increases. The scattering coefficient for particles with diameters comparable with incident wavelengths (*i.e.*, 1 μm) takes values greater than that of other particles sizes. For other size of particles, the scattering coefficient doesn't show considerable variations.

Another dimensionless parameter that plays an important role in the scattering process is the asymmetry parameter (anisotropy). It is defined as the average of cosine over all the scattering angles $< \cos \theta >$ [11] which can be computed as follows

$$Q_{scat} < \cos \theta > = \frac{4}{x^2} \{ \sum_{n=1}^{\infty} \frac{n(n+2)}{n+1} Re(a_n a_{n+1}^* + b_n b_{n+1}^*) + \sum_{n=1}^{\infty} \frac{(2n+1)}{n(n+1)} Re(a_n b_n^*) \}, \quad (21)$$

where the asterisk symbol denotes the complex conjugate of the coefficients.

The scattering anisotropy for three different particle sizes in a specific range of wavelengths is shown in Figure 3B. According to the variations of this parameter, we can see how the scattering made by droplets in various angles is influenced by the particle size. It can be seen that the asymmetry parameter increases with increasing the particle size. For wavelengths much smaller than the particle sizes of interest, the anisotropy reveals a complex behavior. For this sample, the average of the asymmetry parameter is approximately constant in different wavelength limits, but the amount of variance is higher as compared to the other sample sizes.

4   Conclusion

In this study, we presented a simulation of the Mie scattering in the MATLAB environment from droplets floating throughout the atmosphere. In our simulations, the wide range of wavelengths [0.3 1.4 μm] with linear polarization as incident waves were encountered with a surface of different scale of particles which is representative of humidity in the atmosphere. According to Figure 2 and the average of efficiencies, we can say that the scattering efficiency in the Mie scattering rise to a maximum as the particle sizes approach magnitude of the incident wavelength. On the other hand, the back-scattering efficiency in the atmosphere attains its peak value (though with fluctuations) as the diameters of the particles get larger than the incident wavelength. As shown in Section 3, droplet has the greater value of the scattering coefficients for sizes comparable with the incident wavelengths. It means the amount of scattering of these scales of particles in the atmosphere is more than the other sizes. On the basis of our results, the anisotropy of particles that have sizes smaller than wavelengths is much more than the other scales of spheres. Now, we are able to simulate internal and external electromagnetic fields of any kind of spherical non-magnetic particles in the atmosphere by using Mie theory. In the future, we are going to calculate Mie Scattering and related physical parameters of other kind of particles with proximate spherical shapes and different refractive indices existed within the atmosphere.

Acknowledgment

References

[1] Bohren C.F., Huffman D.R., 1983, *Absorption and Scattering of Light by Small Particles*, John Wiley & Sons, Inc.

[2] Mie, G., 1908, Ann. Phys., 25, 377

[3] Debye P., 1909, Ann. Phys., 30, 57

[4] Kerker M., 1969, *The Scattering of Light and Other Electromagnetic Radiation*, Academic, New York

[5] Kreibig U., 2008, Physik in unserer Zeit 39(6), 281

[6] Hergert W., Wriedt T., 2008 *Mie Theory 19082008*, Universität Bremen, Bremen

[7] Horvath H., 2009, J. Quant. Spectrosc. Radiat. Transf., 110(11), 783

[8] Garbin V., Volpe G., Ferrari E., Versluis M., Cojoc D., Petrov D., 2009, New J. Phys., 11(1), 013046

[9] Mishchenko M. I., Quant J., 2009 Spectrosc. Radiat. Transf., 110, 1210

[10] Wriedt T. , 2008, *in Mie Theory 1908−2008*, Universität Bremen, Bremen

[11] Mätzler C., 2002, *MATLAB Functions for Mie Scattering and Absorption*, Research Report No. 2002-08, Institute of Applied Physics, University of Bern

[12] Kolwas M., 2010, Comput. Methods Sci. Technol. 16 Special Issue (2), 108

[13] Yushanov S., Crompton J. S., Koppenhoefer K. S., 2013, *Mie Scattering of Electromagnetic Waves*, Excerpt from the Proceedings of the 2013 COMSOL Conference in Boston

[14] Stratton J. A., Houghton H. G., 1931, *A Theoritical Investigation of the Transmission of Light through Fog*, Physical Review, 38, 159

[15] Houghton H. G., W. R. Chalker, 1949, *The Scattering Cross Section of Water Drops in Air for Visible Light*, Journal of the Optical Society of America, 39, 955

[16] Bayat A., Khalesifard H. R., Masoumi A., 2013, *Retrieval of Aerosol Single-Scattering Albedo and Polarized Phase Function from Polarized Sun-Photometer Measurements for Zanjans Atmosphere*, Atmos. Meas. Tech., 6, 2659

[17] Haberle, R.M., 1998, *Early Mars Climate Models*, J. Geophys. Res., 103, 467

[18] Taylor F. W., et al., 1998, *Investigation of Saturn's Atmosphere by Cassini*, Planet. Space Sci., 46, 1315

[19] García-Cámara B., 2010, *On Light Scattering by Nanoparticles with Conventional and Non-Conventional Optical Properties*, Ph.D. Thesis, Universidad de Cantabria

[20] van de Hulst H. C., 1957, *Light Scattering by Small Particles*, Reprint of the John Wiley & Sons, Inc., New York